The dynamic neptunian ring arcs: evidence for a gradual disappearance of Liberté and resonant jump of courage

Imke de Pater [a,*], Seran G. Gibbard [b], Eugene Chiang [a], Heidi B. Hammel [c], Bruce Macintosh [b], Franck Marchis [a], Shuleen C. Martin [a], Henry G. Roe [d], Mark Showalter [e]

[a] *Astronomy Department, 601 Campbell Hall, University of California, Berkeley, CA 94720, USA*
[b] *Lawrence Livermore National Laboratory, Livermore, CA 94550, USA*
[c] *Space Science Institute, 4750 Walnut Street, Suite 205, Boulder, CO 80301, USA*
[d] *O.K. Earl Postdoctoral Scholar in Planetary Science, Division of Geological and Planetary Sciences, California Institute of Technology, Pasadena, CA 91125, USA*
[e] *STAR Laboratory, Stanford, CA 94305-9515, USA*

Abstract

We present Adaptive Optics observations of Neptune's ring system at 1.6 and 2.2 μm, taken with the 10-m W.M. Keck II telescope in July 2002 and October 2003. We recovered the full Adams and Le Verrier rings for the first time since the Voyager era (1989), and show that the overall appearance of these rings did not change much, except for the ring arcs. Both the location and intensity of all arcs changed drastically relative to trailing arc Fraternité, which has a mean orbital motion of 820.1118 ± 0.0001 deg/day, equal to that of Nicholson et al.'s (1995, Icarus 113, 295–330) solution 2. Our data suggest that all arcs may have decayed over the last decade, while Liberté, in 2003, may be on the verge of disappearing completely. The observed changes in the relative intensities and locations of all arcs further indicate that material is migrating between resonance sites; leading arc Courage, for example, has jumped $\sim 8°$, or, when adopting Namouni and Porco's (2002, Nature 417, 45–47) CER (corotation eccentricity resonance) theory, it advanced by one full corotation potential maximum. Overall, our observations reveal a system that is surprisingly dynamic, and no comprehensive theory exists as of yet that can explain all the observed intricacies.

© 2004 Elsevier Inc. All rights reserved.

Keywords: Planetary rings; Neptune; Infrared observations

1. Introduction

In 1984, three telescopes in South America recorded a partial occultation of a star near Neptune; since the occultation was recorded only on ingress, it was attributed to the existence of a partial ring or ring arc (Hubbard, 1986; Hubbard et al., 1986; Manfroid et al., 1986). The existence of ring arcs around Neptune was confirmed during subsequent years via other occultation experiments (e.g., Nicholson et al., 1990, 1995; Sicardy et al., 1991), and by the Voyager II spacecraft (Smith et al., 1989). The Voyager data established that the Neptunian arcs are concentrations of particles embedded within the narrow Adams ring, the outermost of five tenuous rings discovered by Voyager. These five rings include the relatively bright Adams and Le Verrier rings, the faint Lassell ring (an outward extension of the Le Verrier ring), the Arago ring (the bright outer edge of the Lassell ring), and the innermost ring, the faint Galle ring. Within the Adams ring Voyager identified four ring arcs, confined to a longitude range of 40°, thus confirming the ground-based occultation experiments (Smith et al., 1989; Porco, 1991; Showalter and Cuzzi, 1992; Porco et al., 1995).

---

* Corresponding author. Fax: +1-510-642-3411.
 E-mail address: imke@astron.berkeley.edu (I. de Pater).

Nicholson et al. (1995) analyzed the Voyager images together with ∼ 25 stellar occultations by the Neptune system which were observed from Earth-based telescopes between 1984 and 1988. All observations combined indicated a mean orbital motion of the arcs of either 820.1194 ± 0.0006 deg/day (solution 1) or 820.1118 ± 0.0006 deg/day (solution 2). Solution 1 appeared to be consistent with the existence of a 42:43 resonance between the ring and nearby satellite Galatea, which agreed with Goldreich et al.'s (1986) model for longitudinal confinement of the ring arcs. Such a resonance was attributed to a corotational inclination resonance (CIR) and/or the outer Lindblad resonance between the ring and Galatea (Porco, 1991).

Since Voyager, the ring arcs were imaged with the Near Infrared Camera Multi-Object Spectrograph (NICMOS) on the Hubble Space Telescope (HST) (Dumas et al., 1999) and from the ground with the Canada–France–Hawaii Telescope (CFHT) (Sicardy et al., 1999), both in 1998. None of the continuous rings has been unambiguously recovered in HST or groundbased images. Dumas et al. (2002) derived a mean motion of 820.1122 ± 0.0003 deg/day for the arcs from the HST data, and Sicardy et al. (1999) derived a value of 820.1135 ± 0.0009 deg/day from the CFHT data. Both values are very close to Nicholson et al.'s (1995) solution 2, but clearly discrepant from their solution 1. This finding called into question the theory that the ring arcs are confined by the CIR resonance with Galatea. Namouni and Porco (2002) suggest instead that a resonance based upon Galatea's corotational eccentricity resonance (CER) may be responsible for the confinement of the arcs. This resonance offers 43 potential 'sites' distributed uniformly around the ring orbit where arcs might form, each site having an angular extension of 8.37°.

2. Observations

We observed Neptune and its ring/satellite system on UT 27 and 28 July 2002, and again on UT 3–6 October 2003, with the 10-m W.M. Keck II telescope on Mauna Kea, Hawaii, and its facility instrument NIRC2 (Near-Infrared Camera) coupled to the Adaptive Optics (AO) system (Wizinowich et al., 2000). Neptune's geocentric distance was 29.1 AU in 2002, and 29.6 AU in 2003. The phase angle varied from 0.15°–0.18° in 2002 to 1.64°–1.69° in 2003, while the ring opening angle was −27.7° during both epochs. We used NIRC2 in high angular resolution mode, 0.01″ pixel size, which translates to 210 km/pixel in 2002, and 213 km/pixel in 2003. In 2002, we imaged the neptunian system in K′ (1.95–2.30 μm), in which most of the Sun's light, usually reflected by Neptune's haze layers, is absorbed by methane and hydrogen gas, greatly reducing scattered light around the planet. In 2003, we observed the ring system both in K′ and (on October 5) in H (1.48–1.78 μm). In this paper we focus on the spatial brightness distribution. To enhance the signal-to-noise (SNR) on the rings, we com-

Table 1
Neptune ring data

UT time (yr month day: hr:min)	# frames	Δ (AU)	r_o (AU)	Wavelength band	Phase angle (°)
2002 July 27: 12:04	6	29.078	30.089	K′	0.189
2002 July 27: 12:19	6	29.078	30.089	K′	0.189
2002 July 27: 12:36	6	29.078	30.089	K′	0.188
2002 July 28: 11:43	6	29.077	30.089	K′	0.157
2002 July 28: 12:12	9	29.077	30.089	K′	0.157
2002 July 28: 12:30	6	29.077	30.089	K′	0.156
2002 July 28: 12:53	6	29.077	30.089	K′	0.156
2002 July 28: 13:10	6	29.077	30.089	K′	0.155
2003 Oct. 03: 07:10	5	29.552	30.077	K′	1.633
2003 Oct. 03: 07:27	5	29.552	30.077	K′	1.633
2003 Oct. 03: 07:40	5	29.552	30.077	K′	1.633
2003 Oct. 03: 07:55	5	29.552	30.077	K′	1.633
2003 Oct. 03: 08:02	5	29.552	30.077	K′	1.633
2003 Oct. 03: 08:17	5	29.553	30.077	K′	1.634
2003 Oct. 04: 06:10	5	29.566	30.077	K′	1.649
2003 Oct. 04: 06:25	5	29.566	30.077	K′	1.649
2003 Oct. 04: 08:15	5	29.568	30.077	K′	1.650
2003 Oct. 04: 08:30	5	29.568	30.077	K′	1.650
2003 Oct. 05: 06:10	5	29.581	30.077	H	1.665
2003 Oct. 05: 06:27	5	29.581	30.077	H	1.665
2003 Oct. 05: 06:35	5	29.582	30.077	H	1.665
2003 Oct. 05: 06:51	5	29.582	30.077	H	1.665
2003 Oct. 05: 08:06	3	29.583	30.077	H	1.666
2003 Oct. 06: 06:03	5	29.596	30.077	K′	1.680
2003 Oct. 06: 06:18	5	29.596	30.077	K′	1.680
2003 Oct. 06: 07:32	5	29.597	30.077	K′	1.681
2003 Oct. 06: 07:49	5	29.597	30.077	K′	1.681

Δ = geocentric distance; r_o = heliocentric distance; all images are 1-min integrations in H (1.48–1.78 μm) or K′ (1.95–2.30 μm); the ring opening angle was −27.7°.

bined the K′ and H band data after normalization to the K′ band intensities. We typically took sequences of 5 or 6 1-min exposures, interspersed by the same number of sky frames. A detailed observing log is presented in Table 1. All images were processed using standard near-infrared data reduction techniques (flat-fielded, sky-subtracted, with bad pixels replaced by the median of surrounding pixels). Photometric calibrations were performed on star HD 22686 in 2002, and HD 201941 in 2003 (Elias et al., 1982).

The quality of AO data is usually expressed through the Strehl ratio (SR), and the angular resolution (FWHM, full width at half maximum). The SR is the ratio of the peak intensity of the observed point spread function (PSF) to the theoretical maximum for the telescope aperture. Use of an extended object such as Neptune for AO wavefront sensing may result in a lower SR than usually found for AO observations of stars (e.g., de Pater et al., 2002). This is caused by the fact that extended objects can introduce artifacts in an AO system with a quad-cell Shack–Hartmann sensor, as first noted (for the extreme case of Uranus) in de Pater et al. (2002). The Keck AO team implemented a procedure, suggested by our group, to mitigate this effect prior to the 2003 observations. This led to greatly improved Strehl ratios on extended sources. (See van Dam and Macintosh, 2003, and van Dam et al., 2004 for more discussion.)

We estimated the SR in our data from individual images. We determined the PSF core from images of the satellites Galatea, Larissa and Proteus while using Neptune itself for wavefront sensing. We used separate images of stars to determine the flux in the PSF wings. The SR thus derived most closely resembles the Strehl ratio in our actual Neptune observations. We find a Strehl ratio SR = 0.3 in 2002; in 2003 we find SR = 0.5 at K′, and SR = 0.3–0.4 at H. The FWHM in our images, as measured from the satellite Proteus, which was present in many of our images, is typically between $0.045''$ and $0.055''$ for both our H and K′ band data.

All images were aligned with respect to Neptune to enhance detectability of the continuous rings. We estimate the accuracy of alignment to be better than one pixel. Methods which used one of the inner satellites, such as Proteus, for alignment failed because of inaccuracies in their ephemerides (e.g., Marchis et al., 2004; Jacobson and Owen, 2004). After alignment, the data were combined per day, the results of which are shown in Figs. 1a, 1b, and 1c for 28 July 2002 (K′), 03 October 2003 (K′), and 05 October 2003 (H), respectively. A 1-min exposure of Neptune itself is shown on the inserts, showing detailed structure in its clouds and haze-cover. The atmospheric structure will be discussed in a future paper (see, e.g., Max et al., 2003; Gibbard et al., 2003, and Martin et al., 2004, for discussions regarding previous AO observations of Neptune's atmosphere). The ring images have been high-pass filtered by subtracting the same image median-smoothed with a width of 50 pixels. This procedure removes diffuse scattered light, and brings out small-scale features (Neptune is highly saturated in this presentation). Since the moons and rings are narrow finite structures, the only light that has been lost in this process is that of the (PSF) halo. The error on the final photometry, however, has been minimized by the techniques applied to estimate this halo contribution (Section 3.3). In Fig. 1 we indicated the Adams and Le Verrier rings, as well as the moons Proteus, Larissa, Galatea, and Despina on each panel. The moons trace out a sequence of small arcs on these images by virtue of their individual Keplerian orbital motions.

In order to investigate Neptune's ring arcs quantitatively, we need to combine images to enhance the SNR, since the ring arcs can hardly be seen on single 1-min exposures. Combining 5–6 consecutive images results in too much smearing, as is evident from the satellite arcs in Fig. 1. We therefore deprojected each individual 1-min frame, and before co-adding shifted each one in longitude to correct for the Keplerian motion of the ring arcs. Since this procedure is central to our analysis, we checked each step carefully. For example, we checked our ring deprojection procedure by inserting an artificial Galatea from the JPL ephemeris (NEP022;[1] Owen et al., 1991) in our original image, at 10° intervals along its orbit. Our deprojection procedure resulted in a straight line for artificial Galatea as a function of az-
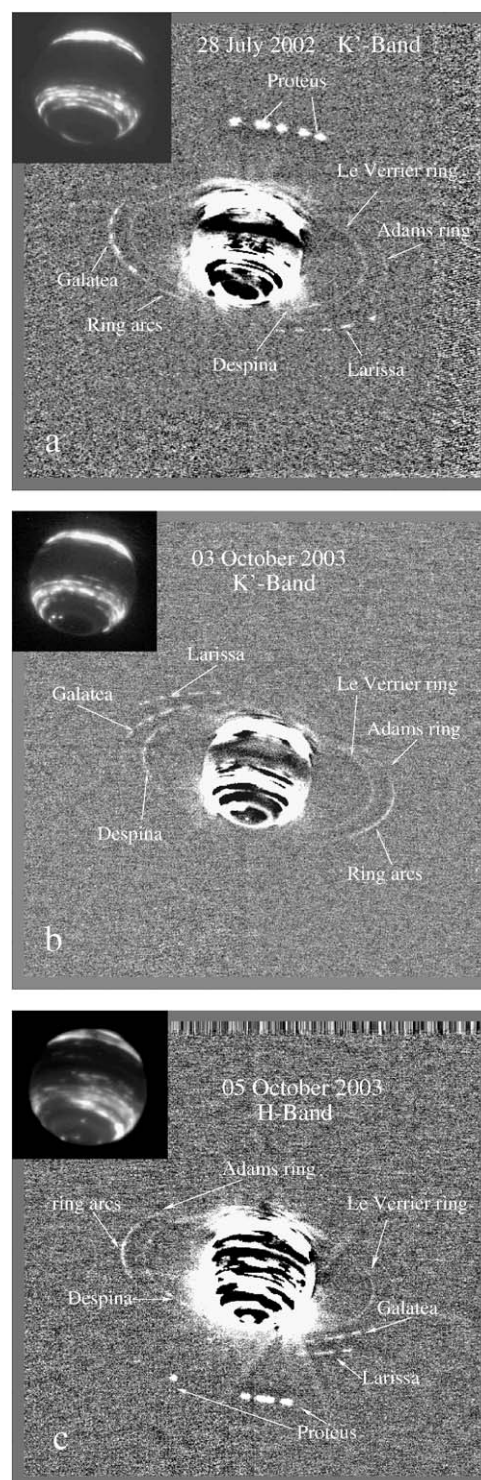

Fig. 1. (a) Average image of the 28 July 2002 data (2.12 μm, 33 min total integration time), revealing satellites, ring arcs and the complete Adams and Le Verrier rings. The images have been high-pass filtered by subtracting the same image median-smoothed with a width of 50 pixels. This procedure removes diffuse scattered light, and brings out small-scale features (Neptune is highly saturated in this presentation). A 1-min exposure of Neptune itself at K′ is shown in the insert. (b) Average high-pass filtered image of the 03 October 2003 data (2.12 μm, 30 min total integration time). The insert shows a 1-min exposure of Neptune itself at K′-band. (c) Average high-pass filtered image of the 05 October 2003 data (1.63 μm, 23 min total integration time). The insert shows a 1-min exposure of Neptune itself at H-band.

---

imuth, where the satellite was visible every 10° in longitude. After deprojection all images were shifted so that Galatea remained fixed in position throughout each day. The differential motion between Galatea and the ring arcs over the course of the observations introduces a longitudinal smear in the images of ∼ 1°, comparable to the angular resolution of our instrument. Since the ring arcs occupied a wide range of locations in azimuth over the course of our observations, we believe that any variations in intensity such as might be caused by different foreshortening effects in viewing geometry are minimal.

3. Results and discussion

3.1. Global appearance of the ring system

The images in Fig. 1 reveal a ring system quite similar to that imaged at visible wavelengths by the Voyager spacecraft (e.g., Smith et al., 1989; Porco et al., 1995). This is the first time that the full Le Verrier and Adams rings have been seen unambiguously in groundbased observations, with Galatea orbiting Neptune just interior to the Adams ring (Fig. 1a), and Despina just interior to the Le Verrier ring (Figs. 1b, 1c). The Le Verrier ring is relatively constant in brightness as a function of azimuth, while the Adams ring is brightest near the ring arcs; 180° away from the ring arcs the Adams ring seems to be faintest. To measure the azimuthal variation quantitatively, we created a longitudinal scan along the Adams ring from the final deprojected image from 03 October 2003, shown in Fig. 2. This scan was obtained by integrating the data in the radial direction over approximately the FWHM of the ring arcs, 0.06″ on this day. Although in-
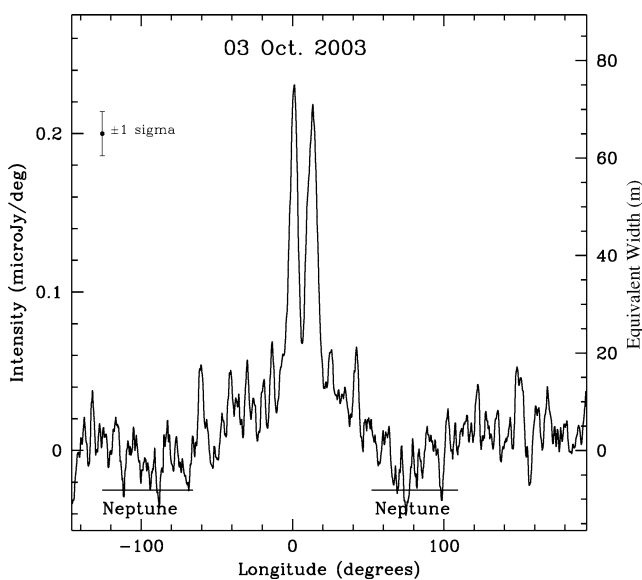

Fig. 2. Longitudinal scan along the Adams ring, obtained from the deprojected image of 03 October 2003. The scan has been integrated in the radial direction over the full extent of the rings, as discussed in the text. Zero longitude was chosen to coincide with the center of arc Fraternité. Equivalent width (in m) is shown on the right.

tegration over the FWHM of the rings results in the highest SNR it does not encompass the full visible thickness of the rings. This requires integration over a width including the full PSF, i.e., encompassing also the PSF halo. The difference between the two numbers is a simple scaling factor. The y-axis on our figures incorporates this correction factor (see Section 3.3) and thus represents the full vertically-integrated intensity of the rings in units of μJy per degree (of longitude). To facilitate comparison with other data, we also calculated the equivalent width, EW, in meters: $EW = \int (I/F)\,dr$, where I is the observed intensity, πF is the solar flux density as reflected from Neptune at the particular wavelength, and r is distance across the arcs. The conversion factor of 1 μJy/pixel is equal to an I/F of 359 km^2. The intensity scale in EW is indicated along the right-hand side of the graph.

The ring brightness in Fig. 2 is slightly suppressed where the ring is closest to Neptune; these regions are indicated on the figure. As shown in Fig. 1, scattered light from Neptune is problematic near the planet. Although our median filtering process did an excellent job recovering the rings even close to Neptune, the scattered light contribution was slightly overestimated, and hence the absolute intensity levels at these longitudes are ignored in this study. The ring brightness varies by a factor of ∼ 3 in azimuth, being maximal near the arcs and minimal ∼ 180° away from the arcs. This is very similar to the maximal brightness variations derived from the Voyager data (Showalter and Cuzzi, 1992; Porco et al., 1995).

A radial profile through the ring system is displayed in Fig. 3. Data were averaged in azimuth for each day, excluding satellites and ring arcs. Profiles for July 2002 and October 2003 are shown in the top two panels, with a combined profile at the bottom. A Voyager profile at a phase angle of 135° is superposed in all panels. The brightness contrast between the Le Verrier and Adams rings is very similar in the Keck and Voyager data, in spite of the very different wavelengths and phase angles. This provides further support for the suggestion, based on the Voyager phase curves, that both rings have similar particle properties (Showalter and Cuzzi, 1992; Porco et al., 1995).

The Voyager spacecraft detected the faint Galle ring at a radial distance of ∼ 41,000 km. Our data, both in 2002 and 2003, may show an enhancement in intensity at this same radial distance. Unfortunately, scattered light from Neptune makes it difficult to detect the Galle ring reliably. It is possible that the elevated intensity levels at the location of the Arago and Lassell rings are caused by the presence of these rings, but the SNR is too low to justify more than hinting at a possible detection.

3.2. Relative changes in the ring arcs

Deprojection and subsequent shifting of the ring images (Section 2) reveal the ring arcs at high signal-to-noise, displayed in Fig. 4a for each epoch individually. In Figs. 4b and 4c we show longitudinal scans. These scans were ob-
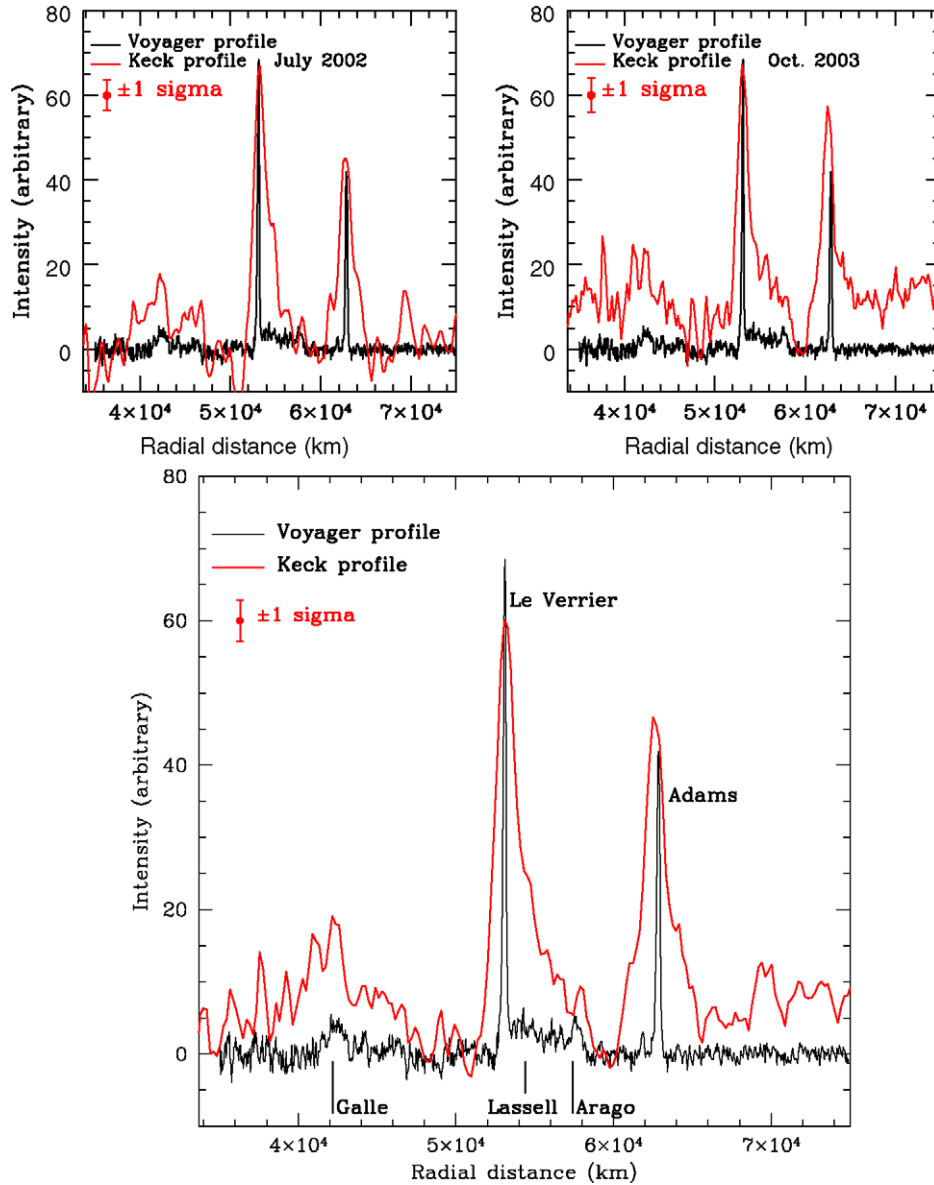
Fig. 3. Radial profiles through the rings. These profiles were obtained by averaging over azimuth on each day, away from satellites and ring arcs. The radial profiles for the 2002 and 2003 epochs are shown in the upper panels, and the combined scan is shown in the lower panel.

tained from Fig. 4a by integrating the data in the radial direction over approximately the FWHM of the arcs: $0.1''$ in July 2002, and $0.06''$ in October 2003. The FWHM in the two years differ due to the substantial improvements in the AO system, discussed in Section 2. Scans at full longitudinal resolution ($\sim 1°$) are shown in Fig. 4b. Although the profiles were obtained by integrating radially over the FWHM of the arcs, the intensity scale on the left represents the integral over the full radial extent of the rings. As in Fig. 2, we show the scale in equivalent width on the right. We superposed a Voyager (1989) profile, scaled to the approximate infrared intensity of arc Fraternité. Figure 4c shows the same scans smoothed to a resolution of $3°$, superposed on the NIC-MOS (1998) data. In the latter figure, the scans have been normalized to the approximate intensity of the Fraternité arc in October 2003. On both graphs we labeled the approximate

location of the various arcs, and indicated the positions of the two subregions, 1 and 2, of arc Egalité. The zero-degree in longitude was chosen to coincide with the center of arc Fraternité. At the Earth received midtime of our observation at 6:37:48 UTC on 05 October 2003, this corresponds to an inertial longitude of $0.5°$, measured from the ascending node of Neptune's ring plane relative to the J2000 Mean Earth Equator. This location coincides with the longitude of Fraternité as predicted by orbit solution #2 of Nicholson et al. (1995) (see Section 3.4).

A comparison of Voyager (1989), NICMOS (1998) and Keck (2002, 2003) profiles in Fig. 4c shows that the relative intensity of most ring arcs has changed dramatically. Compared to arc Fraternité, Egalité has changed both in relative brightness and longitudinal extent (FWHM) since the Voyager flyby. In 2002 Egalité was $\sim 17\%$ brighter than Fra-
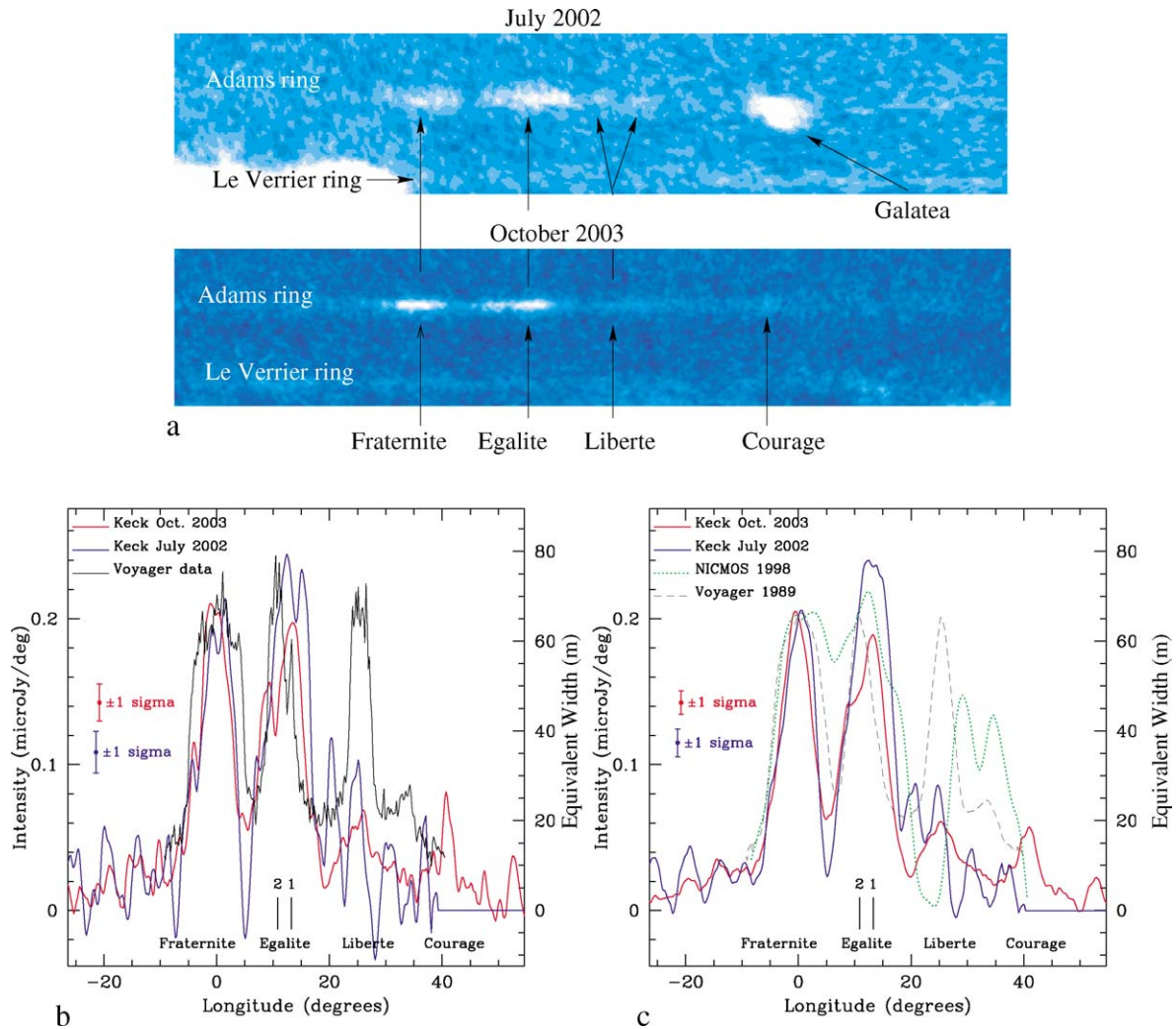
Fig. 4. (a) Deprojected images of the ring arcs from 28 July 2002 (upper panel; 33 min integration time) and all data in October combined (lower panel; 80 min integration time). The image dimensions are $\sim 100°$ in longitude and $\sim 1.1 \times 10^4$ km in radial distance. Since Galatea (upper panel) is much brighter than the ring arcs, this moon, as well as its PSF pattern, are saturated on this display. The PSF pattern around this moon causes Galatea's odd shape. (b) Scans in longitude through the ring arcs from July 2002 and October 2003 at full angular resolution (FWHM is $\sim 1°$), together with a Voyager profile (scaled in intensity to match Fraternité) at a phase angle of 135°. The Keck data were integrated radially over the FWHM of the rings, and the intensity scale was adapted to represent the integral over the full radial extent of the rings (see Fig. 2). Equivalent width (in m) is shown on the right. Zero longitude was chosen to coincide with the center of arc Fraternité. (c) Longitudinal scans through the ring arcs as seen by Keck, Voyager (1989) and NICMOS (1998). The Keck and Voyager profiles were smoothed to a resolution of 3°. All intensities are scaled to that of Fraternité in October 2003. Equivalent width (in m) is shown on the right. Zero longitude was chosen to coincide with the center of arc Fraternité.

ternité ($\sim 3\sigma$), while in 2003 its intensity decreased to $\sim 7\%$ below that of Fraternité ($\sim 2\sigma$), a relative change of $\sim 24\%$ (5σ) in total. In both Keck epochs, as in 1998, Egalité was wider in longitude ($\sim 30\%$ in FWHM) than in 1989. From Fig. 4b it appears that the relative brightness between ring arcs Egalité 1 and 2 is inverted from what Voyager observed in 1989. We note that while Egalité has increased in overall longitudinal extent, the width in azimuth (FWHM) of Fraternité is only 75% that observed by Voyager.

Arc Liberté has continued to decrease in intensity since the NICMOS observations. In 1998, NICMOS showed that Liberté's intensity had decreased roughly by $\sim 25\%$ compared to the Voyager era (relative to Fraternité), and the arc was observed $\sim 3°$ ahead of its longitude. In 2002, our data

suggest that Liberté may consist of two narrow arcs, separated by $\sim 4.5°$, with the leading arc at the original Voyager location. After smoothing the profile to the approximate angular resolution of the NICMOS data (Fig. 4c), the two arcs resemble the double-hump structure observed by NICMOS, but the longitudinal width (FWHM) and location of the Keck profiles suggest the structures differ. In 1998, the NICMOS profile consists of arcs Liberté and Courage (Dumas et al., 1999), whereas in 2002 the Keck double-hump curve is just Liberté. In 2003, Liberté appears again as one arc at the original Voyager (1989) location, at just $\sim 30\%$ of its original brightness (relative to Fraternité).

Courage, usually a low-intensity arc, flared in intensity to become nearly as bright as Liberté when NICMOS ob-

Table 2
Flux densities and reflectivities for Galatea and the ring arcs

	Keck 2002 2.12 μm	Keck 2003 2.12 μm	Keck 2003 1.63 μm	NICMOS 1998[a] 1.87 μm	Voyager 1989[b] 0.5 μm
Galatea flux density (μJy)[c]	5.0±0.8	5.2±0.6	7.1±1	5±2	
Galatea I/F[d]	0.096±0.015	0.094±0.011	0.088±0.012	0.086±0.06	0.079
Arcs (F + E)[e] flux density (μJy)	3.3±0.7	3.6±0.5	5.9±0.9	3.5±0.5	
Scaled[f] arcs (F + E) flux density (μJy)	3.4±0.7	3.6±0.5	3.9±0.6	2.7±0.4	
Arcs (F + E) I/F[g]		0.088±0.012	0.082±0.013	0.083±0.012	0.055
Total[h] scaled arc flux density (μJy)		4.2±0.6		3.6±0.6	

[a] Data from Dumas et al. (2002).
[b] Data from Porco et al. (1995) and Karkoschka (2003).
[c] All uncertainties include a 10% photometric calibration error.
[d] I/F is calculated assuming a 79 km radius for Galatea.
[e] Combined ring arcs Fraternité and Egalité. The 2003 Keck data include a ∼ 0.4 μJy flux density from the (background) Adams ring itself.
[f] Assuming a neutral color for the rings, we scaled the 1.63 and 1.87 μm data according to the Sun's reflectivity (divided the observed flux densities by factors of 1.50 and 1.28, respectively), and Neptune's geocentric and heliocentric distance compared to those on Oct. 3, 2003.
[g] Assumed: 15 km radial extent; 25° in azimuth; normal optical depth $\tau = 0.1$ (Porco et al., 1995). The NICMOS reflectivity is for the entire ring arc system.
[h] Flux density of all arcs combined. The 2003 Keck data include a ∼ 0.5 μJy flux density from the (background) Adams ring itself.

served it in 1998; this flaring was attributed at the time to a possible exchange of material between the two arcs. In 2003, both Courage's and Liberté's intensities had decreased to levels comparable to those of Courage's intensity in 1989. Most interesting is Courage's apparent ∼ 8° shift in the leading direction, as compared to the Voyager era. In terms of Namouni and Porco's (2002) CER model, with 43 potential resonance sites, the arc appears to have 'moved over' in longitude to a potential maximum adjacent to its previous location. If it also was +8° ahead in its orbit in 2002, it was hidden by bright Galatea, which was very close to the ring arcs at that time (Figs. 1a, 4a).

3.3. Absolute photometry

We have shown above that the ring arcs' relative intensities changed dramatically over time. We now investigate if there have been changes in the absolute intensity of the ring arcs to see if the entire ring arc system may be slowly disappearing, or merely the two leading arcs. Since the individual arcs are visible after deprojection and shifting/adding, we used Galatea as a standard calibrator in the deprojected images. The flux density of the satellite Galatea was first determined from our original images, using standard photometric calibrators (Section 2). We note that photometry of adaptive optics images requires an assessment of the amount of light from the observed object that is concentrated in the centermost 0.3″ (the approximate radius of control for the Keck adaptive optics system) and the residual light that is spread into a 'halo' that extends out to an arcsecond or more. We used the procedure as outlined by Gibbard et al. (2004) to capture all Galatea's light.

Galatea's flux density was then used to calibrate the ring arcs in Fig. 4a. Galatea is unresolved in our data, as are the ring arcs in the radial direction. We determined the number of counts for Galatea and the ring arcs by choosing boxes around the objects with the same radial width, and going off the object by the same distance in longitude. Knowing

Galatea's total flux density (including lost halo light), we thus determine the correct total flux density for the ring arcs. All our results are summarized in Table 2. Our derived intensities and reflectivities for Galatea are in excellent agreement with those derived by Dumas et al. (2002). Karkoschka (2003) examined the reflectivities of Neptune's inner satellites from Voyager data (0.55 μm), and determined a geometric albedo of 0.079 for Galatea. Thus we confirm that Galatea is indeed relatively neutral in color, with a slight red excess (see Karkoschka, 2003, for further discussions).

We first examine the absolute intensities of the combined ring arcs Fraternité and Egalité, listed in row 3 of Table 2. We corrected these flux densities for the wavelength variation due to the incident solar flux, assuming the rings are neutral in color, i.e., have a constant albedo between 1.6 and 2.3 μs (row 4, Table 2). The results suggest no significant change between 2002 and 2003, and perhaps a ∼ 25% increase in (scaled) intensity between 1998 and 2002/2003. Assuming a ring arc normal optical depth of 0.1 (Porco et al., 1995), we find a ring reflectivity for Fraternité and Egalité in 2003 of 0.082–0.088 at H–K′ bands (Table 2), in excellent agreement with the NICMOS overall ring arc geometric albedo. Based upon the Voyager measurement of 0.055 ± 0.004 at visible wavelengths (Table 2; Porco et al., 1995) we find that the ring arcs are quite red, in contrast to nearby Galatea. A red color is typical for dusty rings, such as Jupiter's ring (e.g., de Pater et al., 1999) and Saturn's G ring (de Pater et al., 2004).

The flux density from the *entire* ring arc system for the years 1998 and 2003 (row 6, Table 1) suggests that the total flux density of the ring arc system remained unchanged over the last 4 years. Hence, over this period, the decay of leading arcs Liberté and Courage seems to be balanced by a brightening of trailing arcs Fraternité and Egalité.

To compare the ring arc intensities to the 1989 spacecraft data, we selected a Voyager data set at a phase angle of 8° (close to backscattered light). We assume that the overall brightness of the Le Verrier ring has remained constant, and

that the colors of all rings/arcs are the same. This assumption is supported by our observation that the ratio in peak intensities of the Adams (without ring arcs) and Le Verrier rings is similar in the Voyager and Keck data. In the Voyager data the ratio of the intensity averaged over the Fraternité and Egalité arcs to that of the Le Verrier ring is 5.7 ± 0.8. For the October 2003 Keck data we find a ratio of 2.8 ± 0.6. Therefore, given our assumptions, arcs Fraternité and Egalité seem to have decayed over the decade prior to 1998. If true, these ring arcs may slowly disappear over the coming decade(s).

3.4. Mean orbital motions of arcs and Galatea

On all days, the position (centroid) of arc Fraternité coincides exactly with that predicted by Nicholson et al.'s (1995) solution 2, which yields an average mean motion of 820.1118 ± 0.0001 deg/day. The centroid of arc Egalité is just ahead of the position predicted for Voyager (sub-)arc Egalité 2, and appears to be closer to the position of (sub-)arc Egalité 1. This apparent change in brightness structure has probably led Dumas et al. (1999, 2002) to propose a mean motion for the arc system (820.1122 ± 0.0003 deg/day) slightly different from Nicholson et al.'s solution 2.

In 2002, the satellite Galatea is $7.2° \pm 0.5°$ ahead of the nominal longitude predicted from the Voyager-based ephemeris,[2] where the uncertainty is based purely on our own measurements. In October 2003 we find that Galatea is $8.2° \pm 0.5°$ ahead of its nominal position. From this we compute an average mean motion for Galatea of 839.66136 ± 0.00007 deg/day, a value that is in general agreement with the CFHT (839.6613 ± 0.0005 deg/day; Sicardy et al., 1999) and NICMOS (839.6615 ± 0.0004 deg/day; Dumas et al., 2002) observations, and that falls within the uncertainty of the original Voyager-based orbital parameters (839.6598 ± 0.0025 deg/day; Owen et al., 1991). Marchis et al. (2004) have independently derived accurate positions from all our 2002 and 2003 Keck AO data for Proteus, Larissa, Galatea and Despina; these data have been used by Jacobson and Owen (2004) in a larger study to derive an average mean orbital motion of 839.66130 ± 0.00003 deg/day for Galatea.

Our inferred mean motions for the ring arcs and Galatea confirm that the arcs are not at the location of the outer 86:84 corotation inclination resonance (CIR) of Galatea (Porco, 1991). The arcs may be trapped instead in Galatea's 43:42 corotation eccentricity resonance (CER). Although, as pointed out by Namouni and Porco (2002), the CER by itself cannot explain the exact observed mean orbital motion, the CER theory can explain the precise value if the ring arcs' inertia is taken into account. Depending on the arcs'

mass, Galatea's apsidal precession rate can be changed such as to shift the CER exactly onto the arcs' current location. As mentioned before, the CER alone would lead to 43 sites where the arcs can be located, each $8.37°$ in extent, while the CIR generates 86 sites, each $4.18°$ in extent. While both the mean motion of the arcs and the full longitudinal extent of arcs Fraternité ($\sim 10°$) and Liberté ($\sim 8°$) may favor the CER model for confinement, the possible existence of the narrow twin-arcs Liberté in 2002 and the longitudinal extent of Courage ($\sim 2.8°$) suggest that the CIR may still play a significant role, as noted previously by Namouni and Porco (2002). We further note that the overall width of arc Egalité ($\sim 11.5°$) is too large compared to the width of one resonance site in the CER model.

4. Conclusion

We presented Keck Adaptive Optics observations of Neptune's ring system from July 2002 and October 2003. These data show the complete Adams and Le Verrier rings for the first time since the Voyager era. The intensity ratio between the two rings and azimuthal brightness variation within the rings are very similar to those seen in the Voyager data.

Most noteworthy in our datasets are the dramatic changes in the ring arcs. While arc Fraternité appears to follow a well-defined mean orbital motion at 820.1118 ± 0.0001 deg/day, all other arcs shift in location and intensity relative to Fraternité. In particular the leading arcs Liberté and Courage are severely diminished in intensity as compared to the Voyager observations. Voyager (sub-)arcs Egalité 1 and 2 appear to have reversed in relative intensity, perhaps the result of material migrating between resonance sites. Both the 1998 NICMOS and 2002/2003 Keck data indicate that arc Liberté changes resonance sites; if the twin-arc structure seen in 2002 is real, it might represent such a resonance shift in progress. In 2003, Courage was observed $\sim 8°$ ahead in its orbit, i.e., within the CER resonance theory, it had moved over one full resonance site (out of 43 sites).

Occupancy of a given resonance site reflects a balance between interparticle collisions that damp random motions and evacuate the site, and dynamical excitation by Galatea that keeps particles bound to the site (Goldreich et al., 1986). Erosion of a tiny moonlet embedded within the most stable arc, Fraternité, might provide a source population of arc particles. We note that the red color of the ring arcs, as derived in this paper and by Dumas et al. (2002), is consistent with ring arcs being composed of dust, the natural product of moon erosion. If indeed the entire arc system is decaying over as short a timescale as ~ 10 years, as our data suggest, the loss mechanism must, at present, be acting faster than the regeneration mechanism. No quantitative theory has yet been devised that can describe such rapid dynamical evolution.

The mean orbital motion of 820.1118 ± 0.0001 deg/day that we derived for arc Fraternité is equal to Nicholson et

---

[2] The predicted position of Galatea uses JPL ephemeris NEP022 (http://ringmaster.arc.nasa.gov/), based on orbital elements (with a mean orbital motion of 839.6598 deg/day) derived from Voyager data by Owen et al. (1991).

al.'s (1995) solution 2. This finding supports Namouni and Porco's (2002) theory that the ring arcs may be confined by the 43:42 co-rotation eccentricity resonance (CER), which is based upon Galatea's orbital eccentricity. Our data further helped refine Galatea's mean orbital motion to 839.66130 ± 0.00003 deg/day (Jacobson and Owen, 2004). The high precision with which the mean motions of both the ring arcs and Galatea has now been determined can be considered a first step towards future searches for small deviations in the satellite's ephemeris, such as might be caused by a gravitational interaction between Galatea and the ring arcs.

Based upon our findings with regard to the ring arcs, we encourage continued observations of Neptune's ring system to track any future changes. Will indeed some or all ring arcs decay away over time? Or will the full arc system bounce back into existence? Or might it be possible that some arcs re-appear at a completely new location?

Acknowledgments

References

de Pater, I., Martin, S., Showalter, M.R., 2004. Keck 2 μm observations of Saturn's E and G rings during Earth's ring plane crossing in August 1995. Icarus. In press.

de Pater, I., Gibbard, S.G., Macintosh, B., Roe, H.G., Gavel, D., Max, C.E., 2002. Keck adaptive optics images of Uranus and its rings. Icarus 160, 359–374.

de Pater, I., Showalter, M.R., Burns, J.A., Nicholson, P.D., Liu, M.C., Hamilton, D.P., Graham, J.R., 1999. Keck infrared observations of Jupiter's ring system near Earth's 1997 ring plane crossing. Icarus 138, 214–223.

Dumas, C., Terrile, R.J., Smith, B.A., Schneider, G., Becklin, E.E., 1999. Stability of Neptune's ring arcs in question. Nature 400, 733–735.

Dumas, C., Terrile, R.J., Smith, B.A., Schneider, G., 2002. Astrometry and near-infrared photometry of Neptune's inner satellites and ring arcs. Astrophys. J. 123, 1776–1783.

Elias, J.H., Frogel, J.A., Matthews, K., Neugebauer, G., 1982. Infrared standard stars. Astron. J. 87, 1029–1034.

Gibbard, S.G., de Pater, I., Hammel, H.B., 2004. Near-infrared adaptive optics imaging of the satellites and individual rings of Uranus from the W.M. Keck observatory. Icarus. In press.

Gibbard, S.G., de Pater, I., Roe, H.G., Martin, S., Macintosh, B.A., Max, C.E., 2003. Determination of Neptune cloud heights from high-spatial-resolution near-infrared spectra. Icarus 166, 359–374.

Goldreich, P., Tremaine, S., Borderies, N., 1986. Towards a theory for Neptune's arc rings. Astron. J. 92, 490–494.

Hubbard, W.B., 1986. 1981 N1—a Neptune arc? Science 231, 1276–1278.

Hubbard, W.B., Brahic, A., Sicardy, B., Elicer, L.R., Roques, F., Vilas, F., 1986. Occultation detection of a neptunian ring-like arc. Nature 319, 636–640.

Jacobson, R.A., Owen Jr., W.M., 2004. The orbits of the inner neptunian satellites from Voyager, earthbased and Hubble Space Telescope observations. Astron. J. 128, 1412–1417.

Karkoschka, E., 2003. Sizes, shapes and albedos of the inner satellites of Neptune. Icarus 162, 400–407.

Manfroid, J., Haefner, R., Bouchet, P., 1986. New evidence for a ring around Neptune. Astron. Astrophys. 157, L3–L5.

Marchis, F., Urata, R., de Pater, I., Gibbard, S.G., Hammel, H.B., Berthier, J., 2004. Neptunian satellites observed with Keck AO system. In: AAS/DDA Meeting, Nantes, April 2004. Bull. Am. Astron. Soc. 35. Abstract 7.08.

Martin, S.C., de Pater, I., Gibbard, S.G., Marcus, P., Roe, H.G., Macintosh, B.A., Max, C.E., 2004. Adaptive optics imaging of small cloud features on Neptune: zonal wind variability and detections of oscillations in longitude. In: DPS Meeting. Bull. Am. Astron. Soc. 36. Abstract 5.05.

Max, C.E., Macintosh, B.A., Gibbard, S.G., Gavel, D.T., Roe, H.G., de Pater, I., Ghez, A.M., Acton, D.S., Lai, O., Stomski, P., Wizinowich, P.L., 2003. Cloud structures on Neptune observed with Keck telescope adaptive optics. Astron. J. 125, 364–375.

Namouni, F., Porco, C., 2002. The confinement of Neptune's ring arcs by the moon Galatea. Nature 417, 45–47.

Nicholson, P.D., Mosqueira, I., Matthews, K., 1995. Stellar occultation observations of Neptune's rings. Icarus 113, 295–330.

Nicholson, P.D., Cooke, M.L., Matthews, K., Elias, J.H., Gilmore, G., 1990. Five stellar occultations by Neptune. Further observations of ring arcs. Icarus 87, 1–39.

Owen, W.M., Vaughaub Jr., R.M., Synnott, S.P., 1991. Orbits of the six new satellites of Neptune. Astron. J. 101, 1511–1515.

Porco, C.C., 1991. An explanation of Neptune's arcs. Science 253, 995.

Porco, C.C., Nicholson, P.D., Cuzzi, J.N., Lissauer, J.J., Esposito, L.W., 1995. Neptune's ring system. In: Cruikshank, D.P. (Ed.), Neptune. Univ. of Arizona Press, Tucson, AZ, pp. 703–804.

Showalter, M.R., Cuzzi, J.N., 1992. Physical properties of Neptune's ring system. Bull. Am. Astron. Soc. 24, 1029.

Sicardy, B., Roques, F., Brahic, A., 1991. Neptune's rings, 1983–1989: ground-based stellar occultation observations I. Ring-like arc detections. Icarus 89, 220–243.

Sicardy, B., Roddier, F., Roddier, C., Perozzi, E., Graves, J.E., Guyon, O., Northcott, M.J., 1999. Images of Neptune's ring arcs obtained by a ground-based telescope. Nature 400, 731–733.

Smith, B.A., 64 colleagues, 1989. Voyager 2 at Neptune: imaging science results. Science 246, 1422–1449.

van Dam, M.A., Macintosh, B.A., 2003. Characterization of adaptive optics at Keck observatory. In: Proc. SPIE, vol. 5169, pp. 1–10.

van Dam, M.A., Le Mignant, D., Macintosh, B.A., 2004. Performance of the Keck observatory adaptive optics system. Appl. Optics 43, 5458–5467.

Wizinowich, P.L., 17 colleagues, 2000. First light adaptive optics images from the Keck II telescope: a new era of high angular resolution imagery. Publ. Astron. Soc. Pacific 112 (769), 315–319.